frontiers in Earth Science

TYPE Original Research
PUBLISHED 12 May 2026
DOI 10.3389/feart.2026.1799564

# The Southwestern Rift of Africa: isotopic evidence of early-stage continental rifting

Rūta Karolytė[1]*, Michael C. Daly[1], Peter Vivian-Neal[2], Darren Hillegonds[1], Long Li[3], Barbara Sherwood Lollar[4,5] and Chris J. Ballentine[1]

[1]Department of Earth Sciences, University of Oxford, Oxford, United Kingdom, [2]Kalahari GeoEnergy, Lusaka, Zambia, [3]Department of Earth and Atmospheric Sciences, University of Alberta, Edmonton, AB, Canada, [4]Department of Earth Sciences, University of Toronto, Toronto, ON, Canada, [5]Institut de Physiquedu Globe de Paris (IPGP), Université Paris Cité, Paris, France

OPEN ACCESS

EDITED BY
James D. Muirhead,
The University of Auckland,
New Zealand

REVIEWED BY
Zhijie Jia,
Chang'an University, China
Wen Zhang,
Chinese Academy of Geological Sciences, China

*CORRESPONDENCE
Rūta Karolytė,
✉ ruta.karolyte@gmail.com

RECEIVED 30 January 2026
REVISED 08 March 2026
ACCEPTED 16 March 2026
PUBLISHED 12 May 2026

CITATION
Karolytė R, Daly MC, Vivian-Neal P, Hillegonds D, Li L, Sherwood Lollar B and Ballentine CJ (2026) The Southwestern Rift of Africa: isotopic evidence of early-stage continental rifting.
*Front. Earth Sci.* 14:1799564.
doi: 10.3389/feart.2026.1799564

Helium and carbon isotope data ($^3He/^4He$ = 0.14–0.17 $R/R_a$; $\delta^{13}C(CO_2)$ = –3.9‰) from hydrothermal springs within the Kafue Rift of Zambia provide the first geochemical characterization of thermal springs along a broad extensional zone connecting the African Rift System through central Africa to Namibia. These results reveal mantle-derived fluids at the surface, and associated mobilization of crustal $N_2$ (84.4%–97.6%) with elevated $^4He$ concentrations (0.4%–2.3%). Active hydrothermal groundwaters from outside of the Kafue Rift boundary faults show no isotopic evidence of mantle-derived helium or carbon dioxide. These geochemical compositions and spatial trends resemble those observed in other early rifts within the more thermally developed East African Rift System. The data is consistent with early stages of active lithospheric rifting, supported by previous geophysical observations globally. In addition to the regional tectonic importance of these data, these findings highlight the resource potential along central African active fault boundaries. The combination of a mantle fluid source, advective flow along crustal scale fault zones with low level seismicity, and groundwater serving as a sink for mantle $CO_2$ with minimal crustal fluid dilution, indicate potentially favorable conditions for both geothermal energy development and the exploration of economically significant gases in crustal fluids, particularly helium and hydrogen.

KEYWORDS
**East African Rift System (EARS), helium, hydrothermal springs, plate boundary, rifting**

## 1 Introduction

The earliest stages of continental rifting are difficult to identify, as subtle signs of pre-existing lithospheric structural extension and low-level seismicity precede the more recognizable magmatic and structural features that develop in mature systems (Daly et al., 1989; Dunbar and Sawyer, 1996; Lee et al., 2017). Continental rifting nevertheless results in fractional mantle melting, the ascent of mantle-derived fluids, and thermal mobilization of crustal fluids sequestered within cratonic regions, recognizable by fluid $^3He/^4He$ ratio variations (O'Nions and Oxburgh, 1988; Ballentine et al., 1991; Muirhead et al., 2020; Lee et al., 2017). Understanding these nascent phases is critical for uncovering the processes that transform stable lithosphere into active plate boundaries and for exploring associated geothermal (Jolie et al., 2021) and volatile (Danabalan et al., 2022; Ballentine et al., 2025) resources.

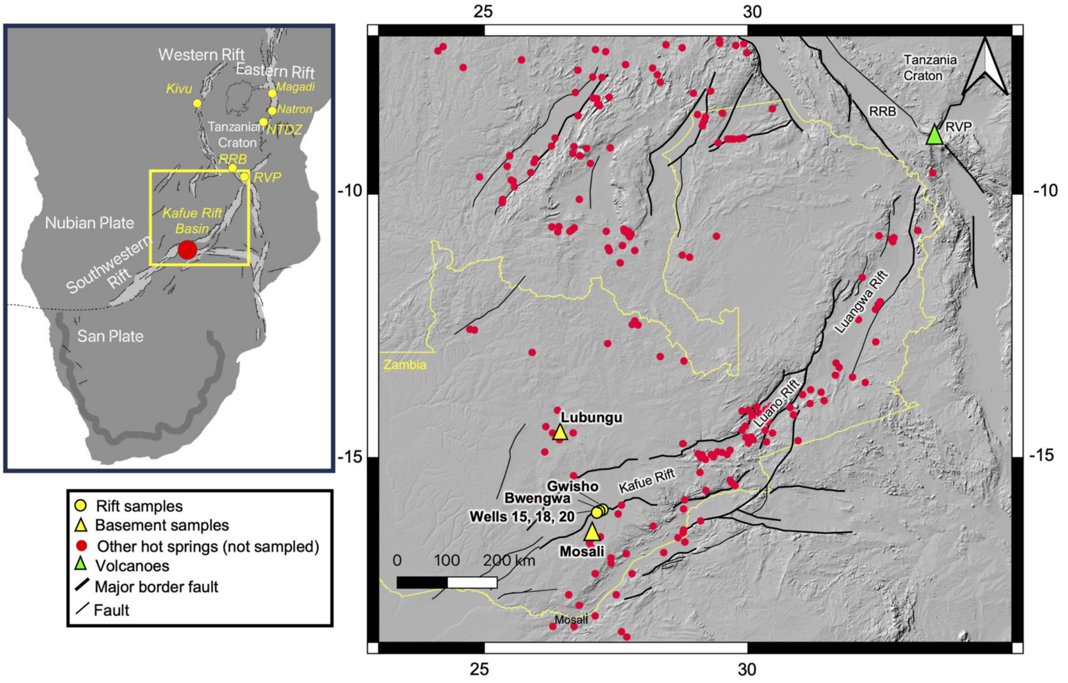

FIGURE 1
Location map (after Daly et al., 2020) of the extensional zone within the Central African Plateau of Zambia. The Kafue Rift is connected to the Luano and Luangwa rifts to the NE, and the Western branch of the EARS at the Rukwa rift (RRB) and Rungwe Volcanic Province (RVP). Rift zone samples include geothermal wells (Well 15, 18, 20) and springs (Bwengwa and Gwisho). Basement hydrothermal spring samples were collected ~50 km to the SW (Mosali spring) and ~150 km to the NNW (Lubungu spring) from the rift zone. Locations of other thermal springs from (Legg, 1974; Tamburello et al., 2022).

Within central Africa, the Kafue Rift in Zambia sits along a contiguous, 2500-km-long active rift faulted zone that may represent a nascent plate boundary (Daly et al., 2020), extending from Tanzania to Namibia and potentially to the mid-Atlantic ridge (Figure 1). The zone is defined by the Luangwa, Luano, and Kafue rifts of Zambia, extending to the Okavango Rift of Botswana and the Eiseb Rift of Namibia. This prospective, Southwestern Rift of Africa boundary is inferred from subtle geomorphology, topographic elements, active fault scarps, low-gravity anomalies, high heat flow, and low-level seismicity (Sebagenzi and Kaputo, 2002; Delvaux and Barth, 2010; Njinju et al., 2019; Wedmore et al., 2021). However, direct geochemical evidence for active mantle-crust interaction has been lacking. If confirmed, it would indicate partitioning of the Nubian Plate from the newly recognized San Plate (Daly et al., 2020), and connect the African Rift System to the Mid-Atlantic Ridge via the Walvis Ridge, which represents a major addition to the framework of African plate dynamics.

By comparing conditions in the Southwestern Rift with the more mature East African Rift System (EARS), we can gauge how early rifting stages evolve toward fully developed rifts. The EARS provides a well-documented reference frame, illustrating a progression from incipient extension, as seen in segments like the Rukwa Rift Basin (RRB) and the Northern Tanzanian Divergence Zone (NTDZ) (Mtili et al., 2021; Kimani et al., 2021; Danabalan et al., 2022) to regions of later stage rifting with active magmatism, such as Rungwe Volcanic Province, Lake Magadi, Lake Kivu (Tedesco et al., 2010; Lee et al., 2017; Pik et al., 2006; Fischer et al., 2009; Kimani et al., 2021; Barry et al., 2013). We assess whether the signals of mantle-crust interaction and early extension, well-documented in the EARS, are manifesting themselves in this proposed Southwestern Rift boundary zone.

## 2 Study area

The Kafue Rift lies within the Central African Plateau of Zambia, bounded by the Congo Craton to the north and the Kalahari Craton to the south (Figure 1). This region is characterized by a local geothermal anomaly in excess of 120 °C/km (Vivian-Neal et al., 2018) and numerous geothermal springs along the broad extensional zone connecting Kafue, Luano, and Luangwa rifts to EARS in Tanzania (Legg, 1974; Tamburello et al., 2022), however only sparse geochemical measurements have been reported. Gas samples were collected from eight geothermal wells and springs across two distinct settings: six fault-related springs and geothermal wells located within the Kafue Rift zone, and two basement-hosted springs Mosali (~50 km SW) and Lubungu (~150 km NNW), situated in the surrounding craton beyond the rift boundary faults.

## 3 Methods

At all sites, free gas was sampled directly from actively bubbling water at the spring or wellhead and collected into refrigeration-grade copper tubes for noble gas analysis, using standard noble gas sampling techniques (Burnard, 2013). Noble gas analysis was conducted in the Noble Laboratory at the University of Oxford using a dual mass spectrometer configuration (Argus VI and Helix SFT), following purification and analytical techniques outlined in (Barry et al., 2016). Helium isotope ratios are reported as $R_c/R_a$, where $R_c$ denotes correction for atmospheric He and $R_a$ denotes the value of air ($1.39 \times 10^{-6}$) (Ballentine and Burnard, 2002a). Radiogenic $^4$He and $^{40}$Ar excesses ($^4He^*$, $^{40}Ar^*$) were calculated using methods outlined in Ballentine and Burnard (2002a). $^4He^*/^{40}Ar^*$production ratios for regional basement rocks were calculated from U, Th and K concentrations (Ballentine and Burnard, 2002a) compiled from global whole-rock geochemical database (Gard et al., 2019), filtered for Precambrian basement samples from Proterozoic mobile belts in the region surrounding the Kafue Rift (n = 250). Major gas concentrations were determined using a quadruple mass spectrometer (QMS) miniRuedi (Brennwald et al., 2016). Gas samples in copper tubes were attached to a 1/16″ stainless steel capillary inlet to the QMS and evacuated to $1 \times 10^{-4}$ mbar. Gas samples were expanded into the analytical volume and pressure was measured using PXM409-USBH pressure transducer. After expansion to the evacuated volume, pressure varied between 0.32–0.5 bar. Gas samples were analyzed for $N_2$, $O_2$, $CO_2$, $CH_4$, and $H_2$, and normalized to a custom laboratory standard of known concentrations. Standards were run at the same pressure range as samples to account for any non-linearity in signal size related to sub-atmospheric pressure. Detection limit (0.1%) was determined experimentally using laboratory standard at relevant pressure range. The total $1\sigma$ error of major gas concentrations incorporating accuracy and reproducibility was 1%. Analyses for stable isotope ratios ($\delta^{15}N$, $\delta^{13}C$) were performed at the University of Alberta using MAT 253 mass spectrometer, following procedure outlined in (Li et al., 2021). Stable isotope ratios ($\delta^{15}N$, $\delta^{13}C$) are reported with respect to V-PDB and air, respectively. The samples are discussed in two groups: the fault-related springs and geothermal wells (referred to as the 'Kafue Rift samples') (n = 6), and basement hosted springs (Mosali and Lubungu springs referred to as the 'basement samples') (n = 2). Full dataset is presented in Supplementary Table S1.

## 4 Results and discussion

The measured $^4$He concentrations range from 0.4 to 2.3 mol% in the Kafue Rift samples, and 0.5–1.3 mol% in the basement spring samples. These values are among the highest observed in hydrothermal fluids within EARS (Figure 2a). The major gas in all samples is $N_2$ (84.4%–97.6%); $O_2$ ranges from 0.1%–6.3%; $CH_4$ was below the detection limit in all samples. The Kafue Rift samples contain 1.5%–15% $CO_2$ while $CO_2$ is below the detection limit in the basement samples (Figure 2b). Helium isotope ratios measured in the Kafue Rift samples exhibit a remarkably consistent signature ranging between 0.14 and 0.17 $R_c/R_A$, while basement spring samples are 0.022 ± −0.002 $R/R_A$ (Figure 2a). Atmospheric $^4$He contribution is negligible in all samples, evidenced by $^4He/^{20}Ne$ ratios ranging from 856–3,240, significantly higher than the air value (0.032). Typical mantle-derived $^3He/^4He$ ratios are around 8 $R/R_A$, while the crustal $^3He/^4He$ production ratio, resulting from thermal neutron capture by $^6$Li, is 0.02 $R/R_A$ (Ballentine and Burnard, 2002a). The Kafue Rift samples exceed the crustal production ratio by a factor of 8, indicating the unambiguous presence of mantle-sourced fluids at the surface. The presence of mantle helium signatures in tectonically active environments without recent magmatism is well-documented (Torgersen, 2010) where elevated tectonic strain rates can create pathways for deep mantle fluids to reach the surface.

The $\delta^{13}C(CO_2)$ value of −3.9‰ measured in a single rift sample (Bwengwa springs-2B) (Table 1) is close to the mantle range (−7 to −4‰) (Wycherley et al., 1999), providing a second line of evidence for surface connectivity to mantle fluids in the Kafue Rift. Such surface expressions of $CO_2$ are characteristic of active extensional tectonic regimes (Sherwood Lollar et al., 1997). $CO_2$ is typically released from the mantle through partial melting of peridotite at depths greater than ~60–70 km (>2 GPa) and temperatures greater than 900 °C (Dasgupta et al., 2022) or through decomposition of carbon-rich melts at shallower depths (<2 GPa), leading to metasomatism and degassing (Frezzotti et al., 2009). These data indicate that fault systems in the Kafue Rift serve as pathways for mantle-derived fluids from zones of partial melting. The preservation of diagnostic mantle $CO_2$ isotopic signatures at the surface demonstrates sustained transport of deep-sourced fluids. When integrated with geophysical observations of lithospheric thinning (Sebagenzi and Kaputo, 2002), this geochemical evidence strengthens the case for active rifting processes.

Nitrogen in crustal fluids can be sourced from the crust (metamorphic, sedimentary) or the groundwater (by equilibration with the atmosphere during water recharge) (e.g., Ballentine and Sherwood Lollar 2002b). Comparing $N_2$ contents to groundwater-sourced $^{20}$Ne allows to differentiate between crustal and groundwater $N_2$ sources. $N_2/^{20}Ne$ ratios of the samples range between 7.5–43 × $10^4$. These samples contain 25%–620% $N_2$ in excess of the dissolved atmospheric component ($N_2/^{20}Ne$ ratios in meteoric water equilibrated with the atmosphere at 25 °C has $N_2/^{20}Ne = 6 \times 10^4$ (Mao and Duan, 2006)). The sole exception is sample Mosali-A, which shows no excess $N_2$, suggesting probable air introduction during sample collection. Overall these results suggests that the major $N_2$ contributor to the rift samples is not atmospheric but crustal rocks, even if the $\delta^{15}N$ values of rift samples (0.2‰–1.6‰) are close to the atmospheric value (0‰) (Figure 2c) but lower than those of crustal rocks (~5‰; see data compilation in (Li et al., 2014)). The slightly lower $\delta^{15}N$ range of $N_2$ in rift samples compared to their crustal source rocks can be reconciled and has been seen elsewhere and attributed to preferential $^{14}$N uptake by $N_2$ during its production, whether it was produced by direct metamorphic $N_2$ degassing from rocks (Bebout and Fogel, 1992) or decomposition of $NH_3/NH_4^+$ in fluids (Li et al., 2009). These interpretations are consistent with the positive relationship between $\delta^{15}N$ and $N_2/^{20}Ne$: as $N_2/^{20}Ne$ increases, the excess $N_2$ with progressively heavier $\delta^{15}N$ fingerprints increasing crustal source input, since crustal rocks (~5‰) are isotopically heavier than the atmosphere (0‰) (Figure 2c). The co-release of radiogenic $^4$He reflects its mobilization from the same basement rocks by the same thermal and tectonic processes, indicating a shared crustal fluid source across the broad zone along the Kafue Rift and within the basement.

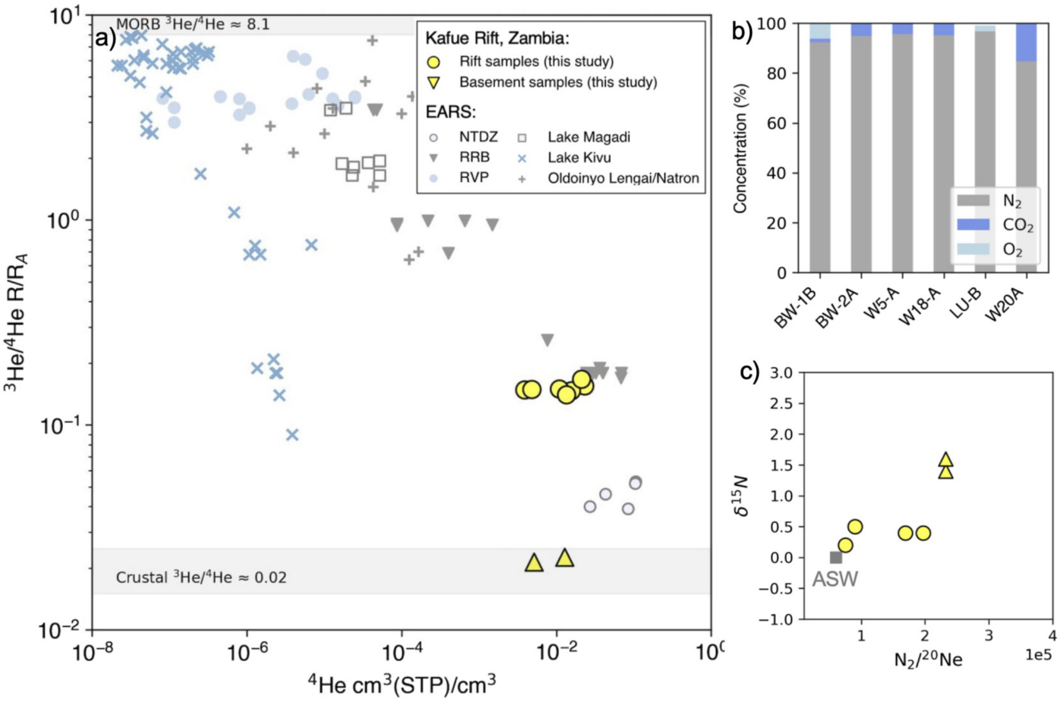

FIGURE 2
**(a)**$^3$He/$^4$He vs. $^4$He concentrations (this study, yellow symbols) compared to hydrothermal fluid observations in the EARS (Tedesco et al., 2010; Fischer et al., 2009; Kimani et al., 2021; Mtili et al., 2021; Barry et al., 2013; Lee et al., 2017; Danabalan et al., 2022; Pik et al., 2006). Hydrothermal fluids near eruptive centres are characterised by high $^3$He/$^4$He ratios and low $^4$He concentrations, while samples distal from the spreading centres are dominated by low $^3$He/$^4$He ratios and high $^4$He concentrations. Zambia rift samples are geochemically similar to observations in NTDZ and RRB. In contrast, Zambia basement samples (yellow triangles) outside of the rift zone are a regional crustal end-member. Full data table in Supplementary Table S2. NTDZ – Northern Tanzanian Divergence Zone; RRB – Rukwa Rift Basin; RVP – Rungwe Volcanic Province. **(b)** $N_2$, $CO_2$, $O_2$ concentrations in Zambia samples. **(c)** $\delta^{15}$N vs. N2/20Ne Samples trend towards more enriched values from air saturated water (ASW).

$^4He^*/^{40}Ar^*$ratios in the Kafue Rift fluids (11–25) (Table 1) are elevated above the average crustal production value of 5.7 ± 2.4 (Ballentine and Burnard, 2002a), but overlap with production ratios calculated from Proterozoic mobile belt basement rocks in the region (median 8.2, IQR 5.7–14, n = 250). Solubility fractionation can be ruled out, based on unfractionated $^{20}Ne/^{36}Ar$ ratios (Supplementary Table 1). $^4He^*/^{40}Ar^*$ratios reflect the geochemical character of the underlying basement, supporting large-scale regional basement degassing. The upper range of measured fluid ratios, which exceed the interquartile range of basement production values, may additionally reflect preferential release of $^4$He relative to $^{40}$Ar at temperatures < 200 °C (Cherniak et al., 2009; Farley, 2000; Harrison et al., 2009), characteristic of shallow hydrothermal systems in early-stage rifts, similar to observations in NTDZ (Danabalan et al., 2022).

The evolution of volatile geochemistry during continental rifting (Figure 3) reflects both the progressive development of mantle-to-surface connectivity and the mobilization of crustal fluids that have accumulated over up to billions of years through water-rock interactions and radioactive processes (Lowenstern et al., 2014; Sherwood Lollar et al., 2014; Danabalan et al., 2022; Ballentine et al., 2025). The Zambian basement samples have purely crustal geochemical signatures with lower $^3$He/$^4$He ratios than any observations in the EARS. This is consistent with earliest stages of rifting, where extension mobilizes crustal fluids through thermophysical changes in the lithosphere, producing compositions that remain close to the basement end-member before mantle fluids enter the hydrological system.

The Kafue rift samples are similar to other early rifting locations in EARS (NTDZ, RRB) (Figure 2a), which exemplify the next stage of development, characterized by $N_2$ as a carrier phase, high $^4$He concentrations (up to 10%), and early stages of mantle fluid admixture (0.04–0.99 R/RA) (Kimani et al., 2021; Mtili et al., 2021; Danabalan et al., 2022). These early-stage signatures develop where active rift zones follow pre-existing basement weaknesses, primarily shear zones between orogenic terranes (Daly et al., 1989), and are associated with initial crustal thinning (Dugda et al., 2005). In the Kafue Rift, this extension is expressed through low-level seismicity and faulting rather than volcanism (Sebagenzi and Kaputo, 2002), consistent with the Western Branch of the EARS rather than the volcanically active Eastern Branch (Yang and Chen, 2010). In more evolved rift segments of both branches (such as Rungwe Volcanic Province, Lake Magadi, Lake Kivu (Pik et al., 2006; Tedesco et al., 2010; Barry et al., 2013; Kimani et al., 2021; Mtili et al., 2021), $CO_2$ later becomes the dominant gas phase as increasing magmatic flux progressively dilutes the early $N_2$-$^4$He signatures (Figure 3c).

This progressive evolution of mantle connectivity is also reflected in $CO_2/^3He$ systematics. While more mature rifts maintain mantle-like $CO_2/^3He$ ratios (1.5 × $10^9$) (Sano and

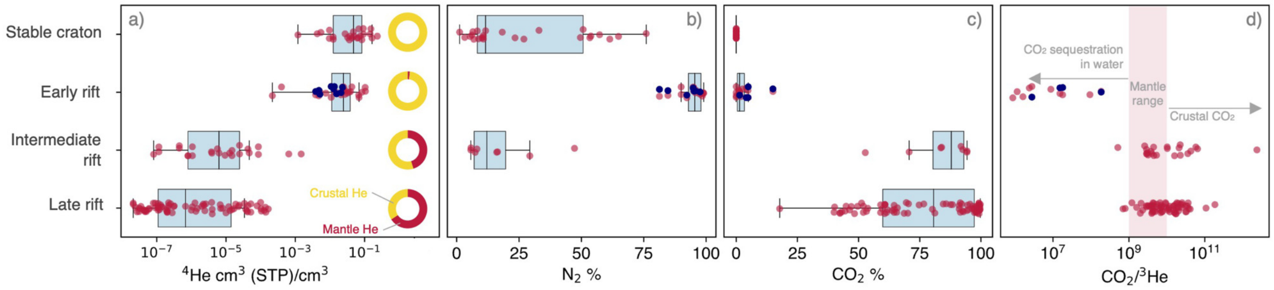

FIGURE 3
Representation of hydrothermal fluid evolution during distinct stages of rifting within the continental crust. Data from Zambia (this study) shown as dark blue circles within the early rift group. The sample sites are grouped into rift stages based on age of rift initiation, lithospheric thickness, and proximity to volcanism. Additionally, we present fracture fluid compositions from stable Archean craton in South Africa (for comparison, as no such data exists in EARS). **(a)** $^4$He concentrations with donut charts illustrating the proportion of crustal (yellow) vs. mantle-derived (red) He contributions at each rift stage. As rifting progresses, crustal signatures are overprinted by mantle helium **(b)** $N_2$ (%) showing dominance of crustal nitrogen in early-stage and stable craton settings, declining with rift maturity. **(c)** $CO_2$ (%) showing progressive increase as rift maturity increases and magmatic flux grows. **(d)** $CO_2/^3He$ ratios; the pink shaded band denotes the mantle range (Sano and Marty, 1995); early-stage rifts plot to the left of this range due to preferential $CO_2$ sequestration in groundwater, while late rifts exceed it due to increasing crustal $CO_2$ input. Data sources: (Tedesco et al., 2010; Fischer et al., 2009; Kimani et al., 2021; Mtili et al., 2021; Barry et al., 2013; Lee et al., 2017; Danabalan et al., 2022; Pik et al., 2006)., and cratonic gases in South Africa (Sherwood Lollar et al., 2006; Karolytė et al., 2022) (full data available in Supplementary Table S2).

Marty, 1995), early-stage settings show significantly lower values due to preferential $CO_2$ loss to groundwater. This is exemplified in the Kafue Rift, where $CO_2/^3He$ ratios range between $2.8 \times 10^6$ and $1.9 \times 10^8$ (Figure 3d, Supplementary Table 1). This reduction occurs where groundwater strips out $CO_2$ more efficiently than helium, and mantle $CO_2$ fluxes are insufficient to maintain a pristine mantle signature. Similar patterns are seen in distal portions of other rift systems, such as the RRB and Egger Graben (Weinlich et al., 1999; Danabalan et al., 2022), where the lower magmatic flux of $CO_2$ is lost to solution, leaving crustal $N_2$ and significant $^4He$ as the dominant major gases. The Kafue Rift's intermediate state, preserving a measurable $CO_2$ component but not a mantle-like $CO_2/^3He$ ratio, and significant crustal $N_2$ and $^4He$, indicates an early-stage rift setting and associated regional crustal fluid mobilization and degassing. Similar $CO_2/^3He$ ratio reductions from mantle-derived fluids interacting with groundwater are observed in other tectonic settings, including convergent margins (Fullerton et al., 2021) and seafloor spreading centers (Walker et al., 2008).

Early stages of continental rifting present unique opportunities for resource exploration, particularly for He, $H_2$, and geothermal energy. Analogous environments with high $N_2$-$^4He$, undiluted by significant mantle $CO_2$ contribution, are particularly promising for helium exploration. $H_2$ is predominantly observed in stable cratons (Lin et al., 2005; Sherwood Lollar et al., 2014; Ballentine et al., 2025) and is less well documented in early rift environments. However, early-stage rifts can show promise for $H_2$ exploration due to their intermediate nature between stable cratons (where $H_2$ accumulation is optimized in ancient fracture-hosted groundwaters), and late rift systems, where $H_2$ is typically lost. Importantly, the low seismic activity in early-stage rifts helps maintain the structural integrity of potential reservoirs. These factors combine to create favorable conditions for the accumulation and preservation of economically significant fluid resources and geothermal energy, making early-stage continental rifts attractive targets for multi-resource exploration efforts.

## 5 Conclusion

This study presents the first geochemical characterization of hydrothermal fluids from the Kafue rift of Zambia, a component of the Southwestern Rift of Africa. Helium isotope ratios (0.14–0.17 Rc/Ra) and $\delta^{13}C(CO_2)$ values close to the mantle range provide evidence of mantle-derived fluids at the surface, accompanied by mobilization of crustal $N_2$ and $^4He$. $CO_2/^3He$ ratios below the mantle range reflect preferential $CO_2$ loss to groundwater, consistent with low magmatic flux at an early rift stage. In contrast, off-rift basement samples exhibit purely crustal geochemical signatures (0.021 R/Ra), indicating that mantle fluid input is restricted to the active fault zones. The absence of volcanic activity and presence of low level seismicity aligns with the Western Branch style of EARS rifting, and these observations closely resemble fluid compositions from early-stage rift segments of the EARS, particularly the NTDZ and RRB. The geochemical results are consistent with an active lithospheric-scale boundary within the Kafue Rift segment. If similar mantle-derived helium anomalies are detected in hydrothermal fluids along other segments of this extensional zone (Luano, Luangwa to NE and Okavango, Eiseb to SW), this would demonstrate that mantle connectivity characterizes the entire boundary zone, providing further compelling evidence for an emerging plate boundary capable of continental separation. Areas in proximity to the plate boundary may be identified as new prospective targets for geothermal and volatile resource exploration, where the combination of mantle fluid input, crustal-scale fault pathways, and low seismicity creates favorable conditions for helium and hydrogen accumulation.

## Data availability statement

The original contributions presented in the study are included in the article/Supplementary Material, further inquiries can be directed to the corresponding author.

## Author contributions

RK: Validation, Writing – review and editing, Formal Analysis, Writing – original draft, Methodology, Data curation, Investigation, Visualization. MD: Resources, Conceptualization, Writing – review and editing, Funding acquisition. PV-N: Writing – review and editing, Resources. DH: Writing – review and editing, Formal Analysis, Methodology. LL: Writing – review and editing, Methodology, Formal Analysis. BS: Formal Analysis, Writing – review and editing. CB: Conceptualization, Writing – review and editing, Resources, Funding acquisition.

## Funding

The author(s) declared that financial support was received for this work and/or its publication. CJB acknowledges support from UKRI [NE/Z000017/1]. CJB and RK acknowledge support from CIFAR (Canadian Institute for Advanced Research). CJB and BSL are Fellows in the CIFAR Earth 4D Subsurface Science and Exploration program.

## Acknowledgements

We thank Geo-Kalahari Energy for granting access to their property and for permission to conduct fieldwork and collect samples.

## Conflict of interest

Author PV-N was employed by Kalahari GeoEnergy.

The remaining author(s) declared that this work was conducted in the absence of any commercial or financial relationships that could be construed as a potential conflict of interest.

## Generative AI statement

The author(s) declared that generative AI was not used in the creation of this manuscript.

Any alternative text (alt text) provided alongside figures in this article has been generated by Frontiers with the support of artificial intelligence and reasonable efforts have been made to ensure accuracy, including review by the authors wherever possible. If you identify any issues, please contact us.

## Publisher's note

## Supplementary material

The Supplementary Material for this article can be found online at: https://www.frontiersin.org/articles/10.3389/feart.2026.1799564/full#supplementary-material

**SUPPLEMENTARY TABLE S1**
Major gas, noble gas, and stable isotope data for fluid samples from the Kafue Rift and off-rift basement sites, Zambia.

**SUPPLEMENTARY TABLE S2**
Literature data compilation (major gas concentrations, helium concentrations and isotope ratios) used in Figures 2 and 3.

## References

Ballentine, C. J., and Burnard, P. G. (2002a). Production, release and transport of noble gases in the Continental crust. *Rev. Mineralogy Geochem.* 47 (1), 481–538. doi:10.2138/rmg.2002.47.12

Ballentine, C. J., and Sherwood Lollar, B. (2002b). Regional groundwater focusing of nitrogen and noble gases into the Hugoton-Panhandle giant gas field, USA. *Geochimica et Cosmochimica Acta* 66 (14), 2483–2497. doi:10.1016/S0016-7037(02)00850-5

Ballentine, C. J., O'Nions, R. K., Oxburgh, E. R., Horvath, F., and Deak, J. (1991). Rare gas constraints on hydrocarbon accumulation, crustal degassing and groundwater flow in the pannonian basin. *Earth Planet. Sci. Lett.* 105 (1–3), 229–246. doi:10.1016/0012-821X(91)90133-3

Ballentine, C. J., Karolytė, R., Cheng, A., Sherwood Lollar, B., Gluyas, J. G., and Daly, M. C. (2025). Natural hydrogen resource accumulation in the Continental crust. *Nat. Rev. Earth & Environ.* 6 (5), 342–356. doi:10.1038/s43017-025-00670-1

Barry, P. H., Hilton, D. R., Fischer, T. P., de Moor, J. M., Mangasini, F., and Ramirez, C. (2013). Helium and carbon isotope systematics of cold "mazuku" CO2 vents and hydrothermal gases and fluids from rungwe volcanic province, southern Tanzania. *Chem. Geol.* 339 (February), 141–156. doi:10.1016/j.chemgeo.2012.07.003

Barry, P. H., Lawson, M., Meurer, W. P., Warr, O., Mabry, J., Byrne, D., et al. (2016). Noble gases solubility models of hydrocarbon charge mechanism in the sleipner vest gas field. *Geochimica Cosmochimica Acta* 194, 291–309. doi:10.1016/j.gca.2016.08.021

Bebout, G. E., and Fogel, M. L. (1992). Nitrogen-isotope compositions of metasedimentary rocks in the catalina schist, California: implications for metamorphic devolatilization history. *Geochimica Cosmochimica Acta* 56 (7), 2839–2849. doi:10.1016/0016-7037(92)90363-N

Brennwald, M. S., Schmidt, M., Oser, J., and Kipfer, R. (2016). A portable and autonomous mass spectrometric system for On-Site environmental gas analysis. *Environ. Sci. Technol.* 50 (24), 13455–13463. doi:10.1021/acs.est.6b03669

Burnard, P. (2013). "The noble gases as geochemical tracers," *Advances in isotope geochemistry* (Springer). doi:10.1007/978-3-642-28836-4

Cherniak, D. J., Watson, E. B., and Thomas, J. B. (2009). Diffusion of helium in zircon and Apatite. *Chem. Geol.* 268 (1–2), 155–166. doi:10.1016/j.chemgeo.2009.08.011

Daly, M. C., Chorowicz, J., and Fairhead, J. D. (1989). Rift basin evolution in Africa: the influence of reactivated steep basement shear zones. *Geol. Soc. Spec. Publ.* 44 (44), 309–334. doi:10.1144/GSL.SP.1989.044.01.17

Daly, M. C., Green, P., Watts, A. B., Davies, O., Chibesakunda, F., and Walker, R. (2020). Tectonics and landscape of the Central African Plateau and their implications for a propagating Southwestern rift in Africa. *Geochem. Geophys. Geosystems* 21 (6), e2019GC008746. doi:10.1029/2019GC008746

Danabalan, D., Gluyas, J. G., Macpherson, C. G., Abraham-James, T. H., Bluett, J. J., Barry, P. H., et al. (2022). The principles of helium exploration. *Pet. Geosci.* 28 (2), petgeo2021–petgeo2029. doi:10.1144/petgeo2021-029

Dasgupta, R., Chowdhury, P., Eguchi, J., Sun, C., and Saha, S. (2022). Volatile-bearing partial melts in the lithospheric and sub-lithospheric mantle on Earth and other rocky planets. *Rev. Mineralogy Geochem.* 87 (1), 575–606. doi:10.2138/rmg.2022.87.12

Delvaux, D., and Barth, A. (2010). African stress pattern from formal inversion of focal mechanism data. *Tectonophysics* 482 (1–4), 105–128. doi:10.1016/j.tecto.2009.05.009

Dugda, M. T., Nyblade, A. A., Julia, J., Langston, C. A., Ammon, C. J., and Simiyu, S. (2005). Crustal structure in Ethiopia and Kenya from receiver function analysis: implications for rift development in eastern Africa. *J. Geophys. Res. Solid Earth* 110 (B1). doi:10.1029/2004jb003065

Dunbar, J. A., and Sawyer, D. S. (1996). Three-dimensional dynamical model of Continental rift propagation and margin Plateau formation. *J. Geophys. Res. Solid Earth* 101 (B12), 27845–27863. doi:10.1029/96jb01231

Farley, K. A. (2000). Helium diffusion from Apatite: general behavior as illustrated by Durango fluorapatite. *J. Geophys. Res. Solid Earth* 105 (B2), 2903–2914. doi:10.1029/1999jb900348

Fischer, T. P., Burnard, P., Marty, B., Hilton, D. R., Füri, E., Palhol, F., et al. (2009). Upper-mantle volatile chemistry at oldoinyo lengai volcano and the origin of carbonatites. *Nature* 459 (7243), 77–80. doi:10.1038/nature07977

Frezzotti, M. L., Peccerillo, A., and Panza, G. (2009). Carbonate metasomatism and CO2 lithosphere–asthenosphere degassing beneath the Western mediterranean: an integrated model arising from petrological and geophysical data. *Chem. Geol.* 262 (1–2), 108–120. doi:10.1016/j.chemgeo.2009.02.015

Fullerton, K. M., Schrenk, M. O., Yücel, M., Manini, E., Basili, M., Rogers, T. J., et al. (2021). Effect of tectonic processes on biosphere–geosphere feedbacks across a convergent margin. *Nat. Geosci.* 14 (5), 301–306. doi:10.1038/s41561-021-00725-0

Gard, M., Hasterok, D., and Halpin, J. A. (2019). Global whole-rock geochemical database compilation. *Earth Syst. Sci. Data* 11 (4), 1553–1566. doi:10.5194/essd-11-1553-2019

Harrison, T. M., Célérier, J., Aikman, A. B., Hermann, J., and Heizler, M. T. (2009). Diffusion of 40Ar in muscovite. *Geochimica Cosmochimica Acta* 73 (4), 1039–1051. doi:10.1016/j.gca.2008.09.038

Jolie, E., Scott, S., Faulds, J., Chambefort, I., Axelsson, G., Gutiérrez-Negrín, L. C., et al. (2021). Geological controls on geothermal resources for power generation. *Nat. Rev. Earth & Environ.* 2 (5), 324–339. doi:10.1038/s43017-021-00154-y

Karolytė, R., Warr, O., van Heerden, E., Flude, S., de Lange, F., Webb, S., et al. (2022). The role of porosity in H2/He production ratios in fracture fluids from the witwatersrand basin, South Africa. *Chem. Geol.* 595 (April), 120788. doi:10.1016/j.chemgeo.2022.120788

Kimani, C. N., Kasanzu, C. H., Tyne, R. L., Mtili, K., Byrne, D., Kazimoto, E., et al. (2021). He, Ne, Ar and CO2 systematics of the rungwe volcanic province, Tanzania: implications for fluid source and dynamics. *Chem. Geol.* 586 (July), 120584. doi:10.1016/j.chemgeo.2021.120584

Lee, H., Fischer, T. P., Muirhead, J. D., Ebinger, C. J., Kattenhorn, S. A., Sharp, Z. D., et al. (2017). Incipient rifting accompanied by the release of subcontinental lithospheric mantle volatiles in the magadi and natron basin, East Africa. *J. Volcanol. Geotherm. Res.* 346, 118–133. doi:10.1016/j.jvolgeores.2017.03.017

Legg, C. A. (1974). *Republic of zambia ministry of mines and industry economic report of the geological survey no. 50 a reconnaissance survey the hot and mineralised springs of zambia by*, 50.

Li, L., Cartigny, P., and Ader, M. (2009). Kinetic nitrogen isotope fractionation associated with thermal decomposition of NH3: experimental results and potential applications to trace the origin of N2 in natural gas and hydrothermal systems. *Geochimica Cosmochimica Acta* 73 (20), 6282–6297. doi:10.1016/j.gca.2009.07.016

Li, L., Zheng, Y.-F., Cartigny, P., and Li, J. (2014). Anomalous nitrogen isotopes in ultrahigh-pressure metamorphic rocks from the Sulu orogenic belt: effect of abiotic nitrogen reduction during fluid–rock interaction. *Earth Planet. Sci. Lett.* 403 (October), 67–78. doi:10.1016/j.epsl.2014.06.029

Li, L., Li, K., Li, Y., Zhang, Ji, Du, Y., and Labbe, M. (2021). Recommendations for offline combustion-based nitrogen isotopic analysis of silicate minerals and rocks. *Rapid Commun. Mass Spectrom.* 35 (10), e9075. doi:10.1002/rcm.9075

Lin, L.-H., Slater, G. F., Sherwood Lollar, B., Lacrampe-Couloume, G., and Onstott, T. C. (2005). The yield and isotopic composition of radiolytic H2, a potential energy source for the deep subsurface biosphere. *Geochimica Cosmochimica Acta* 69 (4), 893–903. doi:10.1016/j.gca.2004.07.032

Lowenstern, J. B., Evans, W. C., Bergfeld, D., and Hunt, A. G. (2014). Prodigious degassing of a billion years of accumulated radiogenic helium at yellowstone. *Nature* 506 (7488), 355–358. doi:10.1038/nature12992

Mao, S., and Duan, Z. (2006). A thermodynamic model for calculating nitrogen solubility, gas phase composition and density of the N2–H2O–NaCl system. *Fluid Phase Equilibria* 248 (2), 103–114. doi:10.1016/j.fluid.2006.07.020

Mtili, K. M., Byrne, D. J., Tyne, R. L., Kazimoto, E., Kimani, C., Kasanzu, C., et al. (2021). The origin of high helium concentrations in the gas fields of Southwestern Tanzania. *Chem. Geol.* 585 (July), 120542. doi:10.1016/j.chemgeo.2021.120542

Muirhead, J. D., Fischer, T. P., Oliva, S. J., Laizer, A., van Wijk, J., Currie, C. A., et al. (2020). Displaced cratonic mantle concentrates deep carbon during Continental rifting. *Nature* 582 (7810), 67–72. doi:10.1038/s41586-020-2328-3

Njinju, E. A., Kolawole, F., Atekwana, E. A., Stamps, D. S., Abdelsalam, E. A., Abdelsalam, M. G., et al. (2019). Terrestrial heat flow in the Malawi rifted zone, East Africa: implications for tectono-thermal inheritance in Continental rift basins. *J. Volcanol. Geotherm. Res.* 387 (December), 106656. doi:10.1016/j.jvolgeores.2019.07.023

O'Nions, R. K., and Oxburgh, E. R. (1988). Helium, volatile fluxes and the development of Continental crust. *Earth Planet. Sci. Lett.* 90 (3), 331–347. doi:10.1016/0012-821X(88)90134-3

Pik, R., Marty, B., and Hilton, D. R. (2006). How many mantle plumes in Africa? The geochemical point of view. *Chem. Geol.* 226 (3–4), 100–114. doi:10.1016/j.chemgeo.2005.09.016

Sano, Y., and Marty, B. (1995). Origin of carbon in fumarolic gas from island arcs. *Chem. Geol.* 119 (1), 265–274. doi:10.1016/0009-2541(94)00097-R

Sebagenzi, M. N., and Kaputo, K. (2002). Geophysical evidences of Continental break up in the south-east of the democratic republic of Congo and Zambia (central Africa). *EGU Stephan Mueller Spec. Publ. Ser.* 2, 193–206. doi:10.5194/smsps-2-193-2002

Sherwood Lollar, B., Ballentine, C. J., and Onions, R. K. (1997). The fate of mantle-derived carbon in a Continental sedimentary basin: integration of CHe relationships and stable isotope signatures. *Geochimica Cosmochimica Acta* 61 (11), 2295–2307. doi:10.1016/S0016-7037(97)00083-5

Sherwood Lollar, B., Lacrampe-Couloume, G., Slater, G. F., Ward, J., Moser, D., Gihring, T., et al. (2006). Unravelling abiogenic and biogenic sources of methane in the earth's deep subsurface. *Chem. Geol.* 226 (3–4), 328–339. doi:10.1016/j.chemgeo.2005.09.027

Sherwood Lollar, B., Onstott, T. C., Lacrampe-Couloume, G., and Ballentine, C. J. (2014). The contribution of the Precambrian Continental lithosphere to global H2 production. *Nature* 516 (7531), 379–382. doi:10.1038/nature14017

Tamburello, G., Chiodini, G., Ciotoli, G., Procesi, M., Rouwet, D., Sandri, L., et al. (2022). Global thermal spring distribution and relationship to endogenous and exogenous factors. *Nat. Commun.* 13 (1), 6378. doi:10.1038/s41467-022-34115-w

Tedesco, D., Tassi, F., Vaselli, O., Poreda, R. J., Darrah, T., Cuoco, E., et al. (2010). Gas isotopic signatures (He, C, and ar) in the Lake Kivu region (western branch of the East African rift system): Geodynamic and volcanological implications. *J. Geophys. Res. Solid Earth* 115 (1), 1–12. doi:10.1029/2008JB006227

Torgersen, T. (2010). Continental degassing flux of $^4$He and its variability: degassing flux of $^4$he and its variability. *Geochem. Geophys. Geosystems* 11 (6), n/a. doi:10.1029/2009GC002930

Vivian-Neal, P., Wilmart, M., Haizlip, J., Hinz, N., Harrison, P., and Sikokwa, S. (2018). "Zambia: Exploration of the non-volcanic, fault hosted Bwengwa River geothermal resource area," in *Proceedings, 7th African Rift Geothermal Conference* (Kigali, Rwanda). Available online at: https://www.cif.org/sites/cif_enc/files/meeting-documents/zambia-exploration_of_bwengwa_river_geothermal_system_accepted_30_sep_2018_id_60999.pdf.

Walker, B. D., McCarthy, M. D., Fisher, A. T., and Guilderson, T. P. (2008). Dissolved Inorganic Carbon Isotopic Composition of Low-Temperature Axial and Ridge-Flank Hydrothermal Fluids of the Juan de Fuca Ridge. *Mar. Chem.* 108 (1–2), 123–136. doi:10.1016/j.marchem.2007.11.002

Wedmore, L. N. J., Biggs, J., Floyd, M., Fagereng, Å., Mdala, H., Chindandali, P., et al. (2021). Geodetic constraints on cratonic microplates and broad strain during rifting of thick southern African lithosphere. *Geophys. Res. Lett.* 48 (17), 1–11. doi:10.1029/2021GL093785

Weinlich, F. H., Bräuer, K., Kämpf, H., Strauch, G., Tesař, J., and Weise, S. M. (1999). An active subcontinental mantle volatile system in the Western Eger rift, central Europe: gas flux, isotopic (He, C, and N) and compositional fingerprints. *Geochimica Cosmochimica Acta* 63 (21), 3653–3671. doi:10.1016/S0016-7037(99)00187-8

Wycherley, H., Fleet, A., and Shaw, H. (1999). Some observations on the origins of large volumes of carbon dioxide accumulations in sedimentary basins. *Mar. Petroleum Geol.* 16 (6), 489–494. doi:10.1016/S0264-8172(99)00047-1

Yang, Z., and Chen, W.-P. (2010). Earthquakes along the East African rift system: a multiscale, system-wide perspective. *J. Geophys. Res. Solid Earth* 115 (B12). doi:10.1029/2009JB006779